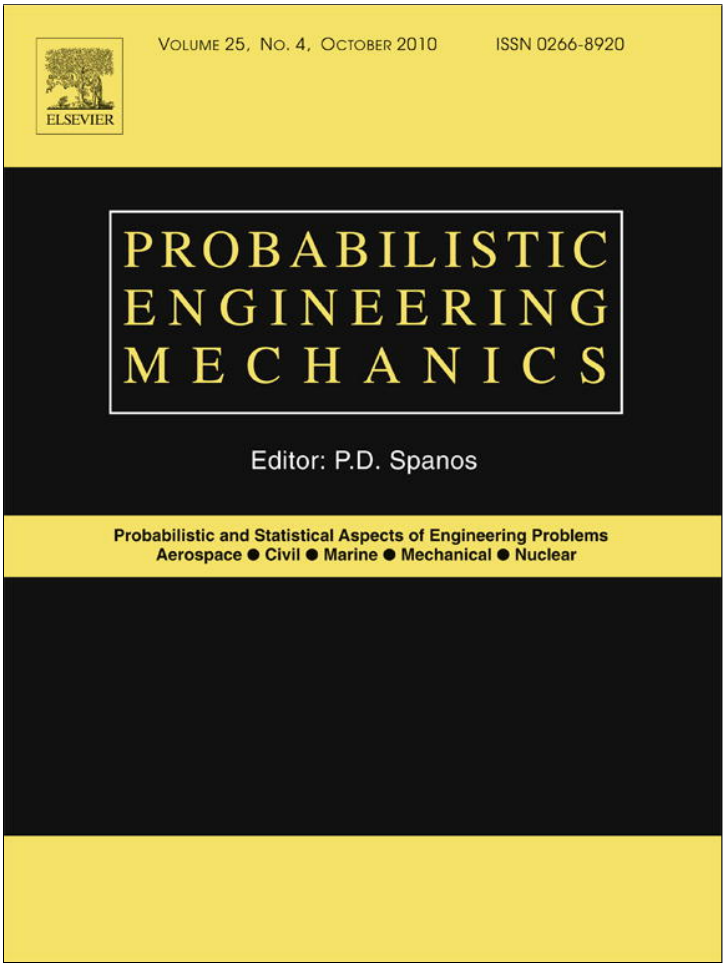
VOLUME 25, NO. 4, OCTOBER 2010
ISSN 0266-8920
ELSEVIER
PROBABILISTIC ENGINEERING MECHANICS
Editor: P.D. Spanos
Probabilistic and Statistical Aspects of Engineering Problems
Aerospace ● Civil ● Marine ● Mechanical ● Nuclear

Probabilistic Engineering Mechanics 36 (2014) 1–7

Contents lists available at ScienceDirect

Probabilistic Engineering Mechanics

journal homepage: www.elsevier.com/locate/probengmech

The asymptotic stochastic strength of bundles of elements exhibiting general stress–strain laws

Marco Salviato, Zdeněk P. Bažant *

Department of Civil and Environmental Engineering, Northwestern University, 2145 Sheridan Road, Evanston, IL 60208, USA

ARTICLE INFO

Article history:
Received 23 July 2013
Accepted 17 January 2014
Available online 24 January 2014

Keywords:
Fiber bundle model
Random strength
Extreme value statistics
Quasibrittle structures
Fracture mechanics
Structural safety

ABSTRACT

The fiber bundle model is widely used in probabilistic modeling of various phenomena across different engineering fields, from network analysis to earthquake statistics. In structural strength analysis, this model is an essential part of extreme value statistics that governs the left tail of the cumulative probability density function of strength. Based on previous nano-mechanical arguments, the cumulative probability distribution function of strength of each fiber constituting the bundle is assumed to exhibit a power-law left tail. Each fiber (or element) of the bundle is supposed to be subjected to the same relative displacement (parallel coupling). The constitutive equations describing various fibers are assumed to be related by a radial affinity while no restrictions are placed on their particular form. It is demonstrated that, even under these most general assumptions, the power-law left tail is preserved in the bundle and the tail exponent of the bundle is the sum of the exponents of the power-law tails of all the fibers. The results have significant implications for the statistical modeling of strength of quasibrittle structures.

1. Introduction

Since the pioneering work by Peirce [1] in the 1920s, the study of fiber bundle models has attracted an increasing attention by the research community. This is due to its proven effectiveness in the analysis of various phenomena across different engineering fields – from material science to earthquake statistics, or from network to traffic modeling, just to mention a few [2–12].

Recently, Kim et al. [2] applied the fiber bundle to study the overloading failures in power grids. The load transfer of broken fibers or nodes through the edges or links of the underlying network was assumed to be governed by the local load-sharing (LLS) rule [13–16].

The same load-sharing rule was adopted by Chakrabarti [3] for the study of (global) traffic jam in a city network of roads. In this case, for some special distributions of traffic handling capacities of the roads, the application of the fiber bundle model let the analytical study of the critical behavior of the jamming transition.

On parallel tracks, Moreno et al. [4] applied the fiber bundle model to study the complex aftershocks sequences which occur after earthquakes. Each element, an asperity or barrier, was supposed to break because of static fatigue, transferring its stress according to a local load-sharing rule and then regenerate.

In material science, the fiber bundle was extensively used as a tool for studying important phenomena such as fracture, fatigue, creep or thermally induced failure of brittle, ductile and quasi-brittle materials [5–12].

Particularly important for structural strength is the asymptotic behavior of the fiber bundle because it governs the extreme value statistics of strength of engineering structures. This is essential for safe design of aircraft, bridges, dams, nuclear structures and ships, as well as microelectronic components and medical implants, since the tolerable failure probability is extremely low, typically $P_f \leq 10^{-6}$.

An early rigorous study of the cumulative probability distribution function (cdf) of the strength and of some asymptotic properties of a fiber bundle with brittle elements (called fibers) was carried out by Daniels [17]. He derived an exact recursive formula for computing the cdf regardless of the particular type of cdf of individual fibers. He also demonstrated that, for the limit case in which the number of fibers approaches infinity, the cdf of strength tends to the Gaussian (or normal) distribution regardless of the cdf of individual brittle fibers. Later, this property was also demonstrated by different approaches by Galambos [18], Smith [19], Sornette [20] and Le et al. [21].

The left tail of the strength distribution for bundles of brittle fibers was studied by Harlow et al. [22] within the framework of set theory. In their work, it was proven in detail that the left tail of the cdf of strength of a fiber bundle is a power-law tail if the elements exhibit a left power-law tail, although this property was already implied in the pioneering work of Fisher and Tippet [23],

* Corresponding author. Tel.: +1 847 491 4025; fax: +1 847 491 4011.
E-mail address: z-bazant@northwestern.edu (Z.P. Bažant).

0266-8920/$ - see front matter
http://dx.doi.org/10.1016/j.probengmech.2014.01.001

in terms of the stability postulate of extreme value statistics. Furthermore, Harlow et al. showed that the tail exponents of brittle fibers are additive, i.e., the exponent of the bundle tail is the sum of the exponents of the power-law tails of all its brittle fibers.

For brittle fibers, the same result was derived by Bažant and Pang [24] in a simpler way using the recursive formula proposed by Daniels [17]. Further, in their paper, the authors demonstrated the presence of a power-law left tail and the additivity of the exponents for ductile fibers. Then they coupled the fiber bundle model to the weakest-link model to describe the multi-scale transition of strength from the nanoscale to the macroscale. They also pioneered the analysis of the reach of power-law tail and showed the reach decreases by one order of magnitude for each element in the bundle. A similar behavior was later demonstrated by Le et al. [21] for fibers characterized by a bilinear stress–strain curve with a gradual post-peak softening.

All the previous analyses of the asymptotic behavior of bundle strength relied on the assumption of a particular constitutive behavior of its elements. In the present work, the constitutive equations describing each fiber are merely assumed to be related by radial affinity while no assumptions are made on their particular form. The cdf of strength of each fiber constituting the bundle is assumed to exhibit a power-law left tail.

It is demonstrated that the power-law left tail is preserved in the bundle. Moreover, it is shown that the exponent is the sum of the exponents of the power-law of each fiber.

2. Preliminary considerations

In the bundle model, after one element fails, the load gets redistributed among the other elements. The total load reduces to zero when all the elements break but the maximum load is reached when only a certain fraction of the elements is subjected to the failure load. The load redistribution after a fiber breaks depends on the load-sharing rule. Various rules have been assumed in the literature, such as the load-sharing by the nearest neighbors of the failing element in the bundle [13–17,25,26].

In the present work, all the fibers are supposed to be subjected to the same relative displacement (note that the more general case of proportional displacements can be transformed to this case). Accordingly, the load-sharing rule is fully determined by the constitutive behavior of the fibers.

The constitutive equations, $s_i = f_i(\varepsilon_i)$, describing the stress–strain law of each ith fiber are supposed to be related by the following affinity:

$$s_0 = \sigma_0 f(\varepsilon) \tag{1}$$

$$s_i = \sigma_i f\left(\beta_i \frac{\sigma_0}{\sigma_i}\varepsilon\right) \quad (i = 1 \ldots n_b) \tag{2}$$

Accordingly, Eq. (1) represents a reference curve while Eq. (2) describes the behavior of each fiber. The parameter σ_i is the strength of the ith fiber, β_i is a positive constant and n_b is the total number of fibers in the bundle. Also, $f(\varepsilon) \in [0,1]$ and it is assumed to have piecewise C^1-continuity in the domain of interest.

It is worth noting that when $\beta_i = 1$, Eqs. (1) and (2) provide a family of curves related by a radial scaling transformation. In case $\beta_i = \sigma_i/\sigma_0$, one gets a vertical scaling. A similar transformation was successfully applied within the framework of the microplane model for the scaling of functions characterizing the constitutive properties of quasibrittle materials [27]. As an example, Fig. 1 shows a family of $\sigma - \varepsilon$ curves describing a material exhibiting a post-peak softening behavior.

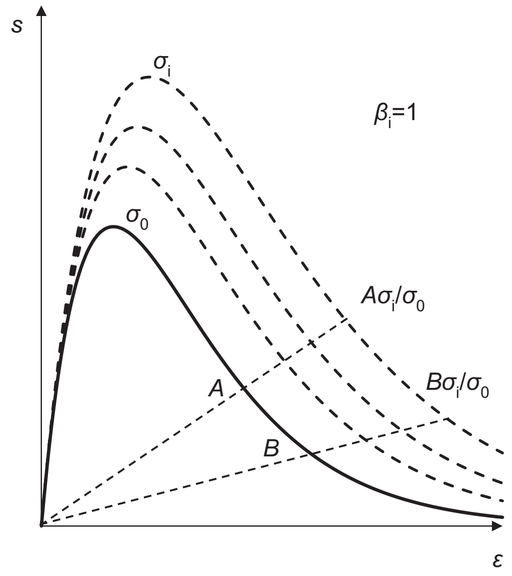

Fig. 1. Example of radially affine stress–strain curves described by Eqs. (1) and (2).

Based on the present assumptions, once the reference curve is defined, each fiber is fully characterized by its strength, σ_i, and its strain at peak, ε_i^*. Note also that no assumptions are made on the particular stress–strain behavior of each fiber. This will guarantee the generality of the results demonstrated in the following sections.

3. Analysis of the left tail of the strength cdf of the fiber bundle

Let us study the tail of the cdf of strength of the fiber bundle model. In contrast to [13–17,25,26], the fibers are supposed to be subjected to the same relative displacement while the load is redistributed within the bundle according to the stress–strain law of each fiber. A surprisingly simple property is demonstrated for power-law tails. The power-laws are always preserved and their exponents are additive. Specifically, if the cdf of strength of each of n_b fibers in a bundle has a power-law tail of exponent p_i ($i = 1 \ldots n_b$), then the cdf of bundle strength has also a power-law tail and its exponent is $p = \sum_{i=1}^{n_b} p_i$.

For a brittle bundle, this remarkable property was proven by induction based on the set theory [22,28]. Later it was also proven more simply by Bažant and Pang [24,29] by means of asymptotic expansion of Daniel's [17] exact recursive equation for the strength of cdf of bundles of increasing n_b. For a plastic bundle, this property was simply proven by induction using the joint probability theorem [24,29]. However, all the previous demonstrations relied on the assumption of a particular stress–strain curve of each element.

For the broad case of fibers with general constitutive behaviors, an analytical proof of the tail exponent additivity has been lacking. It is presented next assuming that each stress–strain curve can be described by an affinity transformation.

3.1. Analytical demonstration

For convenience, the analysis will be initially restricted to two fibers. Then, the demonstration will be extended to the general case of a fiber bundle constituted by n_b fibers.

Consider two fibers and let them be numbered such that $\sigma_1 \le \sigma_2$. Let the only random variables be the peak strengths σ_i (i=1,2) and the ratio σ_1/σ_2 while the reference strength σ_0 and the constants β_1 and β_2 are considered as deterministic quantities characterizing the transformation law.

According to Eqs. (1) and (2), the average stress in the bundle, σ_{avg}, can be written as

$$\sigma_{avg} = \frac{1}{2}\left[\sigma_1 f\left(\beta_1 \frac{\sigma_0}{\sigma_1}\varepsilon\right) + \sigma_2 f\left(\beta_2 \frac{\sigma_0}{\sigma_2}\varepsilon\right)\right] \tag{3}$$

Now, introducing for convenience the change of variable $\varepsilon' = \sigma_0/\sigma_1 \varepsilon$, the peak average stress of the bundle, σ_b, can be written as follows:

$$\sigma_b = \frac{1}{2}\left[\sigma_1 f(\beta_1 \varepsilon') + \sigma_2 f\left(\beta_2 \frac{\sigma_1}{\sigma_2}\varepsilon'\right)\right], \quad \varepsilon' = \varepsilon^* \tag{4}$$

where ε^* is the strain corresponding to the maximum value of average strength. It is worth noting that, due to the randomness of σ_i, ε^* is also a random variable. To show this, first suppose that ε^* is located in a region where $f(\varepsilon)$ has C^1-continuity. Then the average stress of the bundle, σ_{avg}, will satisfy the condition $\partial\sigma_{avg}/\partial\varepsilon' = 0$. This, in view of Eq. (4) leads to the following expression:

$$\beta_1 f'(\beta_1 \varepsilon^*) + \beta_2 f'\left(\beta_2 \frac{\sigma_1}{\sigma_2}\varepsilon^*\right) = 0 \tag{5}$$

It is now clear that ε^* will be a function of the deterministic quantities β_1, β_2 and also of the ratio σ_1/σ_2 which is a random variable. Thus, the maximum average strength of the bundle, Eq. (4), can be rewritten in the following form:

$$\sigma_b = \frac{1}{2}\left[\sigma_1 k\left(\frac{\sigma_1}{\sigma_2}\right) + \sigma_2 w\left(\frac{\sigma_1}{\sigma_2}\right)\right] \tag{6}$$

where $k(\sigma_1/\sigma_2)$ and $w(\sigma_1/\sigma_2)$ are two generic functions of the random ratio σ_1/σ_2. It is important to note that Eq. (6) still holds in the case that the maximum bundle strength is located at a discontinuity point of the general function $f(\varepsilon')$. As can be inferred from Eq. (4), the only difference, should such a case occur, is that k would be a constant.

Now, consider the case when the average bundle strength is less than some prescribed value S:

$$\frac{1}{2}\left[\sigma_1 k\left(\frac{\sigma_1}{\sigma_2}\right) + \sigma_2 w\left(\frac{\sigma_1}{\sigma_2}\right)\right] \le S \tag{7}$$

In such a case, Eq. (7) describes a region $\Omega_2(S)$ in the plane (σ_1, σ_2) whose boundary is determined by the following curve Γ:

$$\Gamma: \quad \sigma_1 k\left(\frac{\sigma_1}{\sigma_2}\right) + \sigma_2 w\left(\frac{\sigma_1}{\sigma_2}\right) = 2S \tag{8}$$

This can be written in parametric form as follows:

$$\Gamma: \quad \begin{cases} t = \dfrac{\sigma_1}{\sigma_2} \\ \sigma_2[tk(t) + w(t)] = 2S \end{cases} \quad t \in [0, 1] \tag{9}$$

which, upon rearranging and introducing the function

$$F(t) = \frac{2}{tk(t) + w(t)} \tag{10}$$

can be rewritten in the following compact form:

$$\Gamma: \quad \begin{cases} \sigma_1 = StF(t) \\ \sigma_2 = SF(t) \end{cases} \quad t \in [0, 1] \tag{11}$$

This system of equations describes the boundary of the region $\Omega_2(S)$ which is shown schematically in Fig. 2. Function $F(t)$ is not known *a priori* and depends on the particular family of the constitutive equations considered. However, since $F(t)$ need not be determined for the following analysis, it suffices to note that, after the parametrization, both σ_1 and σ_2 are expressed as the product of S with a function that does not depend on S. The importance of this result will be evident later.

According to Eq. (7), the strength of each fiber must lie in the domain $\Omega_2(S)$ whose boundary is now described by Eq. (11). Since the strengths of the two fibers are supposed to be independent random variables, the joint probability theorem can be used to express the cdf of the average bundle strength. This provides the following integral equation:

$$G_2(S) = 2\int_{\Omega_2(S)} g_1(\sigma_1) g_2(\sigma_2)\, d\sigma_1\, d\sigma_2 \tag{12}$$

where $g_i(\sigma_i)$ is the probability density function (pdf) of strength of the ith element. This equation has general validity and describes the probability of failure of the bundle for a given stress S.

To study the asymptotic behavior of the distribution, consider the case when S is sufficiently small to guarantee that the strength of each fiber would be within the left power-law tail region. The cdf of strength of the ith element will then be described as $P_i(\sigma) = (\sigma/b_0)^{p_i}$. Then, Eq. (12) can be rewritten as follows:

$$G_2(S) = 2\frac{p_1 p_2}{b_0^{p_1+p_2}} \int_{\Omega_2(S)} \sigma_1^{p_1-1} \sigma_2^{p_2-1}\, d\sigma_1\, d\sigma_2 \tag{13}$$

According to Eq. (11), the region $\Omega_2(S)$ can always be normalized by S without affecting its shape if the transformation $y_i = \sigma_i/S$ is applied. Accordingly, the integral in Eq. (13) can be expressed as

$$G_2(S) = 2\frac{S^{p_1+p_2} p_1 p_2}{b_0^{p_1+p_2}} \int_{\Omega_2(1)} y_1^{p_1-1} y_2^{p_2-1}\, dy_1\, dy_2 = AS^{p_1+p_2} \tag{14}$$

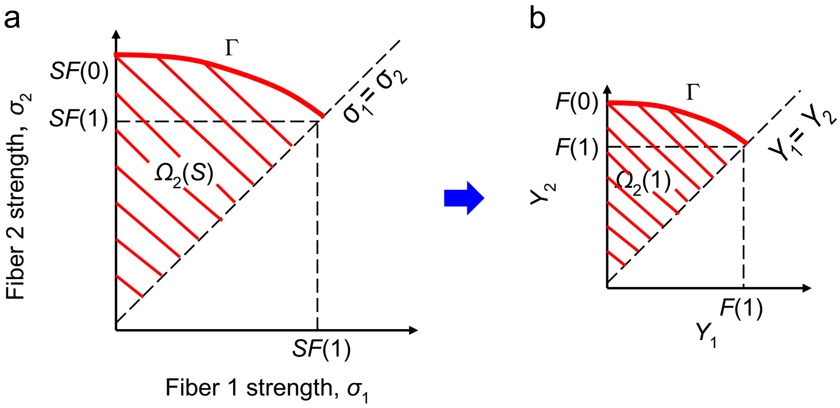

Fig. 2. Schematic of (a) the region $\Omega_2(S)$ of feasible strengths for a fiber bundle composed of two elements and (b) the corresponding region $\Omega_2(1)$ of normalized strengths, $y_i = \sigma_i/S$.

where, for the previous considerations, A is a constant independent on S. This proves that the cdf of bundle strength has a power-law tail whose exponent is p_1+p_2.

By induction, the foregoing analysis can then be easily extended to a bundle with n_b fibers. In this case, the cdf of average bundle strength can be written as

$$G_{n_b}(S) = n_b! S^{p_1+p_2\cdots+p_{n_b}} \int_{\Omega_{n_b}(1)} \prod_{i=1}^{n_b} \left(\frac{p_i y_i^{p_i-1}}{b_0^{p_i}} \right) dy_1\, dy_2 \ldots dy_{n_b} \qquad (15)$$

where the region of feasible strengths of all the fibers, $\Omega_{n_b}(S)$, defines a n_b-dimensional space. $\Omega_{n_b}(1)$ represents the corresponding region of normalized strengths, $y_i = \sigma_i / S$. Since the integral in Eq. (15) does not depend on S, this proves the theory to apply for fiber bundles of any size.

It is worth mentioning here again that S was assumed to be sufficiently small to guarantee the probability of failure of all the fibers to be within the left power-law tail region. This was done because the asymptotic distribution of the bundle strength was of interest. However, Eq. (15) can be numerically integrated to compute $G_{n_b}(S)$ for any strength distribution of the elements of the bundle. Note that, for the case of brittle-elastic fibers, Eq. (15) provides exactly the recursive equation derived by Daniels [17]. For the elastic-perfectly plastic case, Eq. (15) coincides with the equation derived by Bažant and Pang [24]. These can both be considered as particular cases of the present analysis.

It has been proven that the power-law tail is an indestructible property of the bundle provided that the individual fibers exhibit a power-law tail. It has also been shown that the exponent of the power law of the bundle is exactly the sum of the exponents of all the fibers. It is worth mentioning that, for elastic fibers, a similar conclusion was proved by Harlow et al. [22] and Phoenix et al. [28] by using the set theory. The same was also demonstrated by Bažant and Pang [24] for elastic-perfectly plastic fibers, and later by Le et al. [21] for fibers exhibiting a bilinear stress–strain curve with softening behavior. However, all the demonstrations relied on the assumption of a particular constitutive behavior.

This limitation has been overcome here. Since no assumptions are made on the particular stress–strain curve, it has been proven that the indestructibility of the power law tail and the additivity of exponents are general properties of the fiber bundle model with equal relative deformation, the affinity of the stress–strain laws of the individual fibers being the only restriction.

3.2. *Numerical computation of cumulative probability distribution of bundle strength*

To illuminate the results just proven, the strength of a fiber bundle is now numerically computed according to Eq. (15) for an increasing number of fibers. The stress–strain curve of each fiber is supposed to be radially affine ($\beta = 1$) to the curve sketched in Fig. 1 which can be described by the following polynomial expression:

$$s_i = \sigma_i (a x_i^5 + b x_i^4 + c x_i^3 + d x_i^2 + e x_i + f) \mathcal{H}(6 - x_i) \qquad (16)$$

where $x_i = \sigma_0/\sigma_i x$, $\sigma_i =$ strength of the ith fiber, $\mathcal{H}(x)$ represents the Heaviside function and a=0.003, $b = -0.050$, c=0.377, $d = -1.344$, e=1.966 and f=0.021. Eq. (16) is chosen to represent a material that exhibits gradual post-peak softening. This is, for instance, the case for quasi-brittle materials, i.e., brittle materials whose inhomogeneities are not negligible compared to the structure size (exemplified by concrete, fiber composites, or ceramics, among many others).

For convenience, the strength of each fiber is supposed to follow a Weibull distribution with Weibull modulus $p=$ 2 and a scale parameter $b_0 = 1$. This distribution is known to provide a far left power-law tail. However, it should be noted that any cdf of strength exhibiting a left power-law tail could have been assumed.

The numerically computed distribution of the fiber bundle strength is revealed by the Weibull-scale plot in Fig. 3 with increasing n_b. Note that, in this scale, a straight line of slope m represents a power-law tail with exponent m. As can be noted, for all the fiber bundles considered, the cdf of strength reaches a power-law tail represented by different straight lines. In agreement with the present theory, the slope of each line is found to be the sum of the exponents of the fibers constituting the bundle, i.e., $p \times n_b$.

For a higher probability of failure, the cdf of bundle strength begins to deviate slightly from the straight line and approach a different distribution. This behavior was shown for the first time by Daniels [17] who proved that for brittle-elastic bundles the cdf of strength approaches the Gaussian distribution for $n_b \to \infty$ regardless of the cdf of the individual brittle fibers. The same result was later proven within a different framework in [18,20]. A similar conclusion was demonstrated by Bažant and Pang [24,29] for elastic-perfectly plastic fibers. Later, this property was proven for any fiber constitutive law and cdf of strength in [21].

Accordingly, it seems that the right part of the cdf can reasonably be approximated by the Gaussian distribution for a sufficiently high

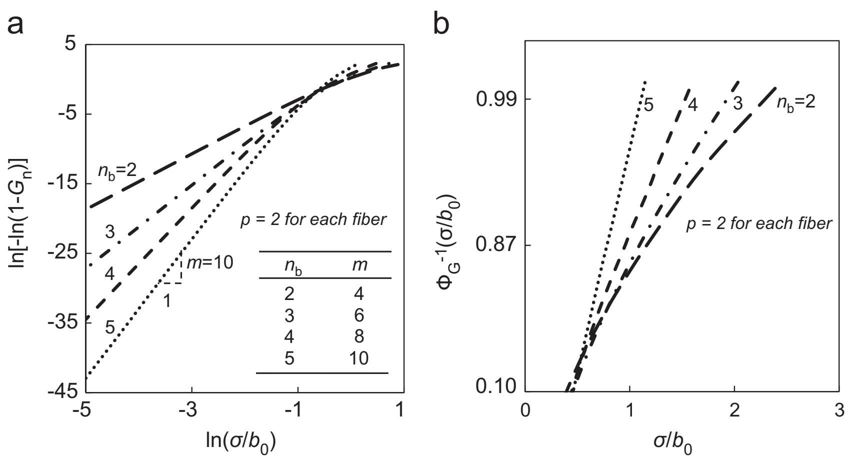

Fig. 3. Strength cdf of fiber bundles with n_b fibers in which each fiber has a Weibull distribution (Weibull modulus $p = 2$). Stress–strain relations are radially affine and described by Eq. (16). (a) Weibull plot for fiber bundles with increasing n_b (a straight line of slope m represents a power law of exponent m); (b) strength cdf of the fiber bundle plotted on Gaussian probability paper (deviation from straight line is a deviation from Gaussian cdf).

number of fibers. This is shown in Fig. 3, where the probability distribution of bundle strength is plotted in the normal (or Gaussian) probability paper. Note that, upon increasing the number of fibers, the distribution approaches a straight line and the approximation by the Gaussian distribution becomes more and more accurate. Also note that the rate of convergence depends on the particular constitutive law of the elements. It was shown that the slowest convergence, of the order of $O(n_b^{-1/3}(\log n_b)^2)$, occurs for brittle bundles [19]. The fastest convergence, of the order of $O(n_b^{-1/2})$, occurs for plastic bundles [24].

4. Implications for hierarchical modeling of structural strength distribution

From atomistic scale arguments, it was shown in [21] that the tail of the cdf of the strength of a nano-scale element must follow a power-law with an exponent equal to 2. This nano-mechanical basis replaces Freudenthal's hypothesis that the strength distribution is determined by the statistics of meso-scale material flaws [30]. Upon careful examination it is found that, in Freudenthal's argument, one set of hypotheses underlying Weibull distribution on the material scale is replaced by another set of equally unverified hypotheses about the statistics of flaws on the meso-scale (in detail see [21,24]).

To relate the strength distributions of a nano-scale element and of a RVE at the macro-scale, a statistical hierarchical model was proposed (Fig. 4); [24,29]. The multi-scale transition relied on two basic statistical approaches: the fiber bundle model and the chain model (or weakest-link model). The idea was that, failing in one link only, the weakest-link model statistically represents the localization of failure within one scale. The fiber bundle model, instead, statistically imposes the condition of compatibility between one scale and its subscale. In other words, it represents the condition that the deformations of several cracked material sub-elements located along the crack path within the fracture process zone must be compatible with the overall deformation of this zone on the higher scale.

The power law tail arising from the nanoscale was shown to be preserved within each scale transition in the RVE. Furthermore, the exponent of the power-law tail was found to increase while passing to higher scales until it reaches its limit value at the RVE scale. These simple tail properties were proven for the particular cases of brittle-elastic and ductile fibers [24], and also for fibers exhibiting a bilinear stress–strain curve with post-peak softening [21].

The present analysis extends the indestructibility of the power-law tail and the additivity of tail exponents to the general case of any fiber bundle model with equal fiber deformations, regardless of the constitutive properties of the fibers. A natural consequence is that the cdf of strength must always exhibit a power law tail. The present analysis also extends to arbitrary constitutive law of fibers another important result demonstrated in [21,24], namely that the strength of one RVE must have a Gaussian distribution transitioning to a power law in the tail of probability within the range of 10^{-4}–10^{-3}:

$$P_1(\sigma) = 1 - \exp\left(-\langle\sigma\rangle^m / b_0^m\right) \quad \text{for } \sigma < \sigma_{gr} \tag{17}$$

$$P_1(\sigma) = P_{gr} + \frac{r_f}{\sqrt{2\pi}\delta_G}\int_{\sigma_{gr}}^{\sigma} e^{-(\sigma' - \mu_G)^2/2\delta_G^2}\, d\sigma' \quad \text{for } \sigma \geq \sigma_{gr} \tag{18}$$

Here $\langle x \rangle = \max(x, 0)$=Macaulay brackets, μ_G and δ_G are the mean and standard deviation of the Gaussian core if considered extended to $-\infty$, b_0 and m are the scale and shape parameters of the Weibull tail, r_f is a scaling parameter required to normalize the grafted cdf such that $P_1(\infty) = 1$, P_{gr} = grafting probability $= 1 - \exp[-\sigma_{gr}^m / b_0^m]$. The continuity of the probability density function at the grafting stress requires that: $(dP_1/d\sigma)|_{\sigma_{gr}^+} = (dP_1/d\sigma)|_{\sigma_{gr}^-}$ where P_1 denotes the failure probability of one RVE.

Note that the RVE must here be defined as the smallest material volume whose failure triggers the failure of the entire structure and must not be confused with the RVE definition in classical micro-mechanics of materials without softening damage [24,29]. Also note that we have in mind only failures under load control conditions, and only the broad class of structures of positive geometry, which are those that become unstable as soon as macro-crack propagation initiates from one RVE.

The localization and inter-scale compatibility conditions are not the only reason why the RVE must be modeled by a hierarchy of series and parallel couplings [24,29]. Another reason, identified in [24], is that the parallel coupling of two fibers shortens the

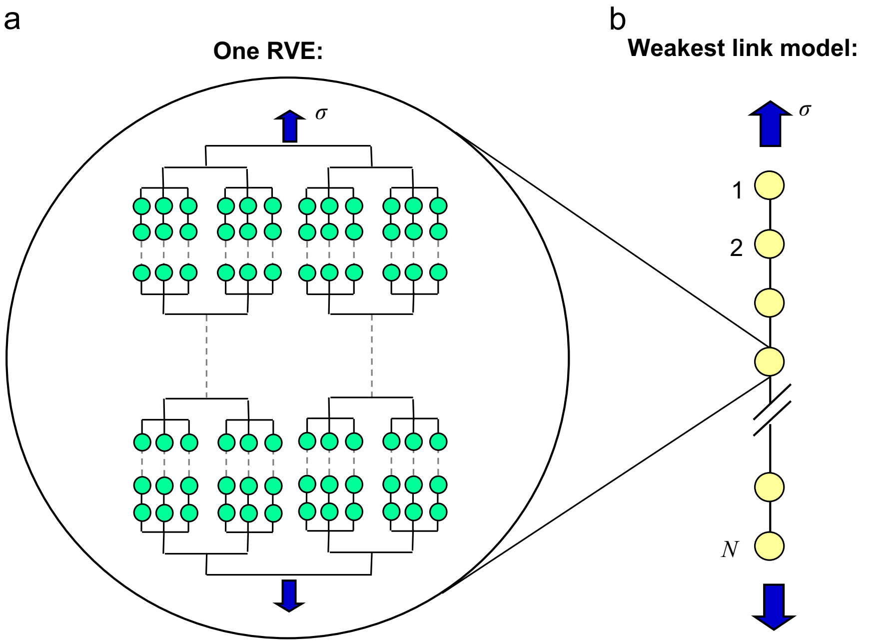

Fig. 4. (a) Hierarchical model representing one RVE; (b) weakest link model representing a structure of any size.

probability reach of the power law-tail by about one order of magnitude, and that extending a chain by a factor of 10 extends the probability reach by about one order of magnitude. Thus, if the RVE were modeled only by parallel couplings, the power-law tail on one RVE would be so remote that the Weibull distribution and scaling could never be observed on any real structure.

To give an idea of how the foregoing results can be applied to strength statistics, some examples are presented next. Attention is focused on the broad class of quasibrittle materials for which the RVE size is not negligible compared to the structure dimensions. In this case, the cdf of structural strength transitions from Gaussian to Weibullian depending on the structure size and shape [21,24].

5. Examples of application of hierarchical model to cdf of strength of quasibrittle structures

Attention is now focused on the broad class of structures exhibiting the so-called positive geometry, i.e., structures that fail under controlled load as soon as a macro-crack initiates from one RVE. This implies that the structure is statistically equivalent to a finite chain of RVEs coupled in series (Fig. 4). Then, according to the joint probability theorem, the cdf of structural strength can be derived from the statistics of one RVE, i.e., from Eqs. (17) and (18):

$$P_f(\sigma_N) = 1 - \prod_{i=1}^{N} \{1 - P_1[\langle \sigma_N s(\mathbf{x}_i) \rangle]\} \tag{19}$$

where $\sigma_N =$ nominal strength of the structure, $s(\mathbf{x}) =$ dimensionless stress field such that $\sigma_N s(\mathbf{x}_i) =$ maximum principal stress of the ith RVE at the position $\mathbf{x}_i$, and N=number of the statistical RVEs in the structure.

Figs. 5a–c show an example of optimum fits of the strength histograms of some engineering quasibrittle materials by means of Eqs. (19) and (17) and (18).

Fig. 5a shows some strength histogram tests of Lanthanum-glass-infiltrated alumina glass ceramics reported in [31]. This material is very attractive for restorative dentistry due to its aesthetics and bio-compatibility as well as its high strength and fracture toughness. Alumina-glass composites consisting of dry-pressed and pre-sintered α-Al_2O_3 with a medium grain size were tested. All alumina were CAD/CAM machined into prisms with dimension 3 $\times$ 4 $\times$ 45 mm before infiltration with 25% (by weight) of glass. 27 four-point bending specimens were tested, under dry conditions.

Another example of optimum fit of strength is provided in Fig. 5b showing the data reported in [32] for a single Nicalon fiber embedded in a silicon carbide matrix. This material is used as fibrous reinforcement in many ceramic composites for high temperature applications. In this case, the investigated specimens consisted of approximately 45%, by volume, of Nicalon fibers in an eight harness satin (8-HS) weave construction, with about 20%, by volume, of CVI Sic matrix. Three-point bending fracture toughness tests of chevron-notch specimens of approximate dimensions of $5 \times 5 \times 50$ mm were conducted. The direction of load application was always perpendicular to the fiber laminae while the strength distribution of a single fiber was determined from the analysis of each fracture mirror.

The optimum fit of strength data reported in [33] for the broad class of unidirectional glass-epoxy composite materials is also shown in Fig. 5c. In this case, the specimens were 19 mm wide $\times$ 191 mm long with gauge length of 114 mm. Each analyzed specimen consisted of eight unidirectional plies and 71 tests were performed.

Despite the relatively low number of tested specimens, Figs. 5a–c clearly show that the strength histograms plotted in Weibull scale are not straight lines, as would be required by the two-parameter Weibull distribution. In fact, the Weibull scale histograms consist of two parts separated by a relatively abrupt kink, the presence of which can be demonstrated only combining the hierarchical and the weakest-link models [21,24]. As shown by the solid curves, the grafted Gauss–Weibull distribution, Eq. (19) and (Eqs. 17) and (18), gives a very good fit, considering the scatter of the data for all the investigated quasibrittle materials. This is not surprising since, according to the derivations in the preceding sections, the main assumptions behind the Gauss–Weibull distribution coupled to the Finite Weakest-Link Theory can be applied to any material, no matter its constitutive behavior. This has also been extensively validated by fitting strength histograms of a great variety of materials [21,24,29].

Finally, note that a three-parameter Weibull distribution is physically unacceptable. By reverse scale transitions it would imply a finite threshold for the activation energy controlled jumps on the atomistic scale, which is impossible. Also, the three-parameter Weibull distribution gives an incorrect size effect, a fact typically overlooked. In detail, see [21,24].

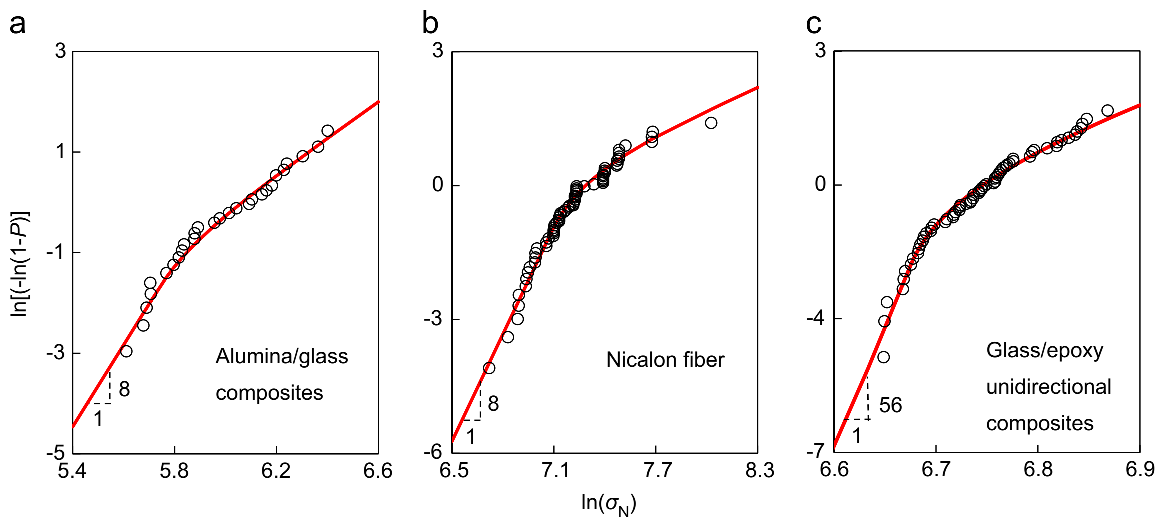

Fig. 5. Optimum fits of strength histograms of some engineering materials: (a) alumina/glass composites [31], (b) single Nicalon fiber in silicon carbide matrix [32] and (c) glass/epoxy unidirectional composites [33]. σ_N in MPa.

6. Conclusions

In the present work, the tail of the strength distribution of a bundle is studied assuming an equal deformation rule. Based on previous atomistic arguments, the distribution of strength of each fiber constituting the bundle is considered to exhibit a power law left-tail. Supposing that the constitutive equations describing each fiber are related by an affinity, it is demonstrated that

1. the power-law left tail is preserved,
2. the tail exponent is the sum of the exponents of the power-law tails of each fiber,
3. These asymptotic properties of the fiber bundle model have general validity since no assumptions are made on the particular constitutive behavior of each fiber.

These results have significant implications for statistical modeling of the strength of quasibrittle structures.

Acknowledgement

Support under NSF grant CMMI-1153494 and ARO grant W911NF–0-1-0043, both to Northwestern University, is gratefully acknowledged.

References

[1] Peirce FT. Tensile tests for cotton yarns, part v: the weakest link theorems on the strength of long and composite specimens. J Text Ind 1926;17:355–368.
[2] Kim D-H, Kim BJ, Jeong H. Universality class of the fiber bundle model on complex networks. Phys Rev Lett 2005;94 025501:1–4.
[3] Chakrabarti BK. A fiber bundle model of traffic jams. Physica A 2006;372:162–166.
[4] Moreno Y, Correig AM, Gómez JB, Pacheco AF. A model for complex aftershock sequences. J Geophys Res 2001;106:6609–6619.
[5] Mishnaevsky Jr L, Brøndsted P. Micromechanical modeling of damage and fracture of unidirectional fiber reinforced composites: a review. Comput Mater Sci 2009;44:1351–1359.
[6] Alava MJ, Nukala PKVV, Zapperi S. Statistical models of fracture. Adv Phys 2006;55:349–476.
[7] Kun F, Zapperi S, Herrmann HJ. Damage in fiber bundle models. Eur Phys J 2000;17:269–279.
[8] Michlmayr G, Or D, Cohen D. Fiber bundle models for stress release and energy bursts during granular shearing. Phys Rev E 2012;86 061307:1–7.
[9] Turcotte DL, Newman WI, Shcherbakov R. Micro and macroscopic models of rock fracture. Geophys J Int 2003;152:718–728.
[10] Camata G, Corotis R, Spaccone E. Simplified stochastic modeling and simulation of unidirectional fiber reinforced composites. Probab Eng Mech 2004;19:33–40.
[11] Pradhan S, Chakrabarti BK. Failure properties of fiber bundle models. Int J Mod Phys B 2003;17:5565–5581.
[12] Pradhan S, Hansen A, Chakrabarti BK. Failure processes in elastic fiber bundles. Rev Mod Phys 2010;82:499–555.
[13] Harlow DG, Phoenix SL. The chain-of-bundles probability model for the strength of fibrous materials II: a numerical study of convergence. J Compos Mater 1978;12:314–334.
[14] Phoenix S-L. The asymptotic time to failure of a mechanical system of parallel members. SIAM J Appl Math 1978;34(2):227–246.
[15] Phoenix S-L. Stochastic strength and fatigue of fiber bundles. Int J Fract 1978;14(3):327–344.
[16] Smith RL, Phoenix SL. Asymptotic distributions for the failure of fibrous materials under series-parallel structure and equal load-sharing. J Appl Mech 1981;48:75–82.
[17] Daniels HE. The statistical theory of the strength of bundles and threads. Proc R Soc Lond A 1945;183:405–435.
[18] Galambos J. The asymptotic theory of extreme order statistics. New York: Wiley; 1978.
[19] Smith RL. The asymptotic distribution of the strength of a series-parallel system with equal load sharing. Ann Probab 1982;10:137–171.
[20] Sornette D. Elasticity and failure of a set of elements loaded in parallel. J Phys A 1989;22:243–250.
[21] Le J-L, Bažant ZP, Bažant MZ. Unified nano-mechanics based probabilistic theory of quasibrittle and brittle structures: I. Strength, static crack growth, lifetime and scaling. J Mech Phys Solids 2011;59:1291–1321.
[22] Harlow DG, Smith RL, Taylor HM. Lower tail analysis of the distribution of the strength of loadsharing systems. J Appl Probab 1983;20:358–367.
[23] Fisher RA, Tippett LHC. Limiting forms of the frequency distribution of the largest and smallest member of a sample. Proc Camb Philos Soc 1928;24:180–190.
[24] Bažant ZP, Pang S-D. Activation energy based extreme value statistics and size effect in brittle and quasibrittle fracture. J Mech Phys Solids 2007;55:91–134.
[25] Phoenix SL, Tierney L-J. A statistical model for the time dependent failure of unidirectional composite materials under local elastic load-sharing among fibers. Eng Fract Mech 1983;18:193–215.
[26] Mahesh S, Phoenix SL, Beyerlein IJ. Strength distributions and size effects for 2D and 3D composites with Weibull fibers in an elastic matrix. Int J Fract 2002;115:41–85.
[27] Bažant ZP, Xiang Y, Prat P. Microplane model for concrete. I: stress–strain boundaries and finite strain. J Eng Mech 1996;122:245–254.
[28] Phoenix SL, Ibnabdeljalil M, Hui C-Y. Size effects in the distribution for strength of brittle matrix fibrous composites. Int J Solids Struct 1997;34:545–568.
[29] Bažant ZP, Pang S-D. Mechanics based statistics of failure risk of quasibrittle structures and size effect on safety factors. Proc Natl Acad Sci USA 2006;103 (25):9434–9439.
[30] Freudenthal AM. Statistical approach to brittle fracture. In: Liebowitz H, editor. Fracturean advanced treatise. New York: Academic Press; 1968. p. 591–619.
[31] Lohbauer U, Petschelt A, Greil P. Lifetime prediction of CAD/CAM dental ceramics. J Biomed Mater Res 2002;63:780–785.
[32] Eckel AJ, Bradt RC. Strength distribution of reinforcing fibers in a Nicalon fiber/chemically vapor infiltrated silicon carbide matrix composite. J Am Ceram Soc 1989;72:455–458.
[33] Hahn HT, Kim RY. Proof testing of composite materials. J Compos Mater 1975;9:297–311.